Molecular Mobility in Cyclic Hydrocarbons: A Simulation Study

Heiko Schmitz, Roland Faller, and Florian Müller-Plathe*

Max-Planck-Institut für Polymerforschung, Ackermannweg 10, 55128 Mainz, Germany

Received: March 3, 1999; In Final Form: June 15, 1999

Mixtures of cyclohexane and cyclohexene are investigated by means of all-atom molecular dynamics simulations. Thermodynamic properties (density, enthalpy of vaporization), transport coefficients (different diffusion coefficients, reorientation times), and structural properties (radial distribution functions) were calculated for seven different compositions and compared to experimental results where available. Transport coefficients indicate a nonideal behavior at low cyclohexene concentrations. The problem of determining the mean-squared displacement from a constant pressure simulation is addressed, and a method is derived, which minimizes the artifacts introduced by the rescaling of the periodic box.

Introduction

Atomistic molecular dynamics simulation has turned out to be a powerful tool in the analysis of the thermodynamics and the microscopic structure of liquids.[1−4] The simulated microscopic trajectory allows direct access to structural properties such as radial distribution functions or transport coefficients, such as diffusion coefficients and the reorientation times of bond vectors, which are often difficult to observe in experiments. The method is based on a semiempirical force field, which has to be adapted to every single substance on the basis of experimentally observed quantities if a high accuracy and reliability is desired. It has been applied very successfully to various one-component organic liquids, but only few all-atom simulations of organic−organic or organic−inorganic mixtures have been reported.[5−7] Since it is well-known that binary mixtures show a rich variety of interesting thermodynamic effects,[8] it is promising to investigate them theoretically with modern simulation methods. We simulated seven different mixtures of the chemically similar liquids cyclohexane and cyclohexene as an example. The force fields have been constructed for the pure liquids. Thermodynamic properties, such as density and enthalpy of vaporization, are used to check their transferability to mixtures. Radial distribution functions give insight into the structure of the mixtures. The *inter*- and *intra*diffusion coefficients as well as the reorientation times of molecular bond vectors were calculated. They show some correlation of the molecular transport.

This paper is organized as follows: In section 2.1 the technical details of the simulation are presented, 2.2 deals with the definition of diffusion coefficients in mixtures, 2.3 addresses the problem of the calculation of the mean-squared displacement in an *NpT* ensemble. Section 3 shows the results for thermodynamic properties, liquid structure, diffusion coefficients, and reorientation times.

2. Simulation and Data Analysis

2.1. Details of the Simulation. Different mixtures of cyclohexane (C_6H_{12}) and cyclohexene (C_6H_{10}) were simulated at ambient conditions ($T = 300$ K, $p = 1013$ hPa). We investigated seven systems, which contained either 250 or 256 molecules (Table 1). The mixtures with only six molecules of one kind allow the extrapolation of the interdiffusion coefficient to the limit of zero concentration.

The molecular dynamics package YASP[9] was used to run the all-atom simulations under constant pressure (Berendsen manostat with coupling time $\tau_p = 2$ ps) and constant temperature (Berendsen thermostat[10] with $\tau_T = 0.2$ ps at a time step of 2 fs. The cutoff for nonbonded interactions was $r_c = 0.9$ nm with a Verlet neighbor list[11] cutoff of 1 nm. No charges were taken into account.

In an atomistic simulation, a detailed force field is necessary to represent the structure and the internal degrees of freedom of the molecules as well as the intermolecular forces. Since the geometric structure of small molecules is well-known (from, for example, microwave experiments) bond lengths, bond angles, and dihedral angles are available. These force field parameters were taken from former simulations,[12] see Table 2.

On the other hand, values for the nonbonded Lennard-Jones parameters have to be estimated from similar substances and then reoptimized individually. This is usually a lengthy procedure, which has to be done manually. We used an algorithm, which automatically adapted the Lennard-Jones parameters to the experimental values of density and enthalpy of vaporization by the simplex method.[12] It saves manpower and gives more accurate results than the traditional trial-and-error approach.

The system was prepared as follows: The appropriate number of molecules was put at random positions and orientations in a large periodic box (about half the real density). This system was simulated for short intervals at a time step that started from 0.001fs and was increased to 1 fs. At the latter value the simulation was run until total energy and density had equilibrated, which took several hundred picoseconds.

After the equilibration the systems were simulated for 1−3.5 million time steps (2−7 ns of real time).

2.2. Diffusion coefficients in pure and mixed liquids. The diffusion coefficients are calculated from the mean-squared displacements of the centers of mass of the molecules via the Einstein relation

$$D \approx \langle \Delta r^2 \rangle / 6t \qquad (1)$$

Theoretically, eq 1 becomes exact in the limit $t \rightarrow \infty$. Practically, the slope of the mean squared displacement is calculated in the

10.1021/jp990761s CCC: $18.00
Published on Web 10/12/1999

TABLE 1: The Simulated Systems

	C_6H_{12}	C_6H_{10}	N	$x(C_6H_{10})$	t^{sim}[ns]
1	250	0	250	0.000	2.0
2	250	6	256	0.023	2.0
3	192	64	256	0.250	3.3
4	125	125	250	0.500	7.2
5	64	192	256	0.750	4.0
6	6	250	256	0.977	2.0
7	0	250	250	1.000	2.0

[a] The second and the third column are the numbers of molecules of the indicated species, N is the total number of molecules. t^{sim} is the total simulation time.

TABLE 2: Geometry and Force Field Parameters of Cyclohexane and Cyclohexene[a]

parameter		C_6H_{10}	C_6H_{12}
Atomic Masses [u]			
H	m	1.00787	1.00787
C	m	12.01	12.01
Bond Lengths r[nm]			
C_1-C_2	r	0.1334	0.1526
C_6-C_1, C_2-C_3	r	0.1500	0.1526
C_3-C_4, C_5-C_6	r	0.1520	0.1526
C_4-C_5	r	0.1540	0.1526
$C_{sp2}-H$	r	0.1080	
$C_{sp3}-H$	r	0.1090	0.1090
Angle potential ϕ_0 [deg], k_ϕ [kJ/(mol rad^2)]			
C−C−C	ϕ_0	110.0	109.5
	k_ϕ	450	335
C=C−C	ϕ_0	112.0	
	k_ϕ	500	
$C_{sp2}-C-C$	ϕ_0	123.45	
	k_ϕ	450	
C−C−H	ϕ_0	109.5	109.5
	k_ϕ	500	420
$C-C_{sp2}-H$	ϕ_0	119.75	
	k_ϕ	500	
H−C−H	ϕ_0	109.5	109.5
	k_ϕ	500	290
Harmonic Dihedrals δ_0[deg], k_δ [kJ/(mol rad^2)]			
C−C=C−C	δ_0	0	
	k_δ	250	
H−C=C−C	δ_0	180	
	k_δ	200	
Torsions (periodicity $p = 3$), τ_0[deg], k_τ [kJ/mol]			
C−C−C−C	τ_0	180	
	k_τ	10	
Lennard−Jones Parameters ϵ[kJ/mol], σ[nm]			
H	ϵ	0.265	0.189
	σ	0.252	0.258
C_{sp3}	ϵ	0.296	0.299
	σ	0.311	0.328
C_{sp2}	ϵ	0.296	
	σ	0.321	

[a] See ref 9 for their definitions.

linear regime. The criterion for the linear regime in our analysis was that the *local exponent*

$$E_n = \ln(\Delta r_{n+1}^2/\Delta r_n^2)/\ln(t_{n+1}/t_n) \qquad (2)$$

was in the interval (0.9; 1.1), which was fulfilled in a large range starting after some 10 pico seconds and ending at about one-third of the total simulation time, where statistical fluctuations become too large (see Figure 1).

In pure liquids, there is only one diffusion coefficient, the self-diffusion coefficient defined by eq 1. In mixtures, things become more complex.[13] The *intra*diffusion coefficients are defined as in eq 1, but the average is taken over one species

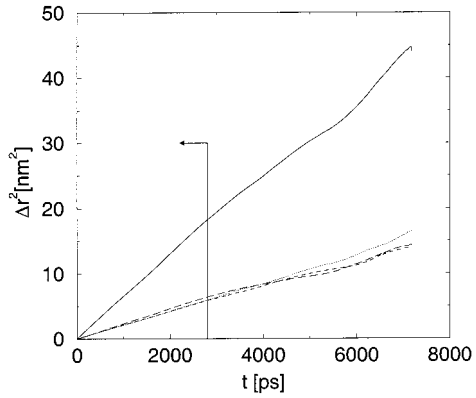

Figure 1. Figure 1. Mean-squared displacement in x, y, z direction and total of cyclohexane in mixture 4; the line indicates the end of the linear regime.

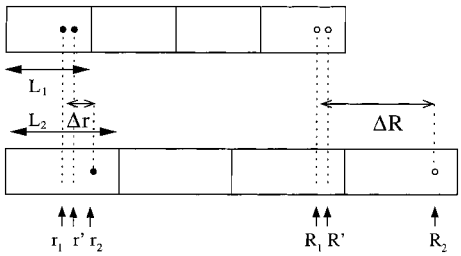

Figure 2. Displacement of particles and their periodic images (schematic).

only. The *inter*diffusion coefficient is calculated from the mean squared displacement of the center of mass of all molecules of one species with an additional prefactor:

$$D_i^{inter} = x_1 x_2 \left(\frac{1}{x_1 M_1} + \frac{1}{x_2 M_2}\right)^2 (x_i M_i)^2 \frac{N\langle(\Delta r_i^{cm})^2\rangle}{6t} \qquad (3)$$

N is the total number of particles, x_1 and x_2 are the mole fractions of species 1 and 2, and M_1 and M_2 are their molecular weights. If the center of mass of the complete system does not move, i.e., if momentum is conserved, $D_i^{inter} = D_2^{inter}$ and eq 3 defines a unique interdiffusion coefficient.[13]

2.3. Calculation of the Mean-Squared Displacement in *NpT* Simulations. In our simulations of an *NpT* ensemble with a Berendsen manostat, the calculation of Δr^2 is nontrivial for the following reason: The manostat rescales all coordinates in every step with a factor s depending on the difference between actual pressure and target pressure. This means an unphysical displacement of the atoms, which depends on their *absolute* positions, thus destroying translational invariance. The displacement Δr of a particle must not depend on the actual periodic image we look at. This is sketched in one dimension (see Figure 2). A particle starts at the position r_1 with a box length L_1. First, the forces move it by Δr_f to $r' = r_1 + \Delta r_f$; then the box and the coordinates are scaled by $s = L_2/L_1$, so that the final position is $r_2 = sr'$. The naive displacement, i.e., the difference of the coordinates, is $\Delta r = r_2 - r_1 = (\Delta L/L_1)r_1 + (L_2/L_1)\Delta r_f$, where $\Delta L = L_2 - L_1$. The relative changes of the box length $\Delta L/L_1$ are usually small, and the second term is just the rescaled displacement Δr_f. However, the first term is proportional to the absolute value of r_1. A periodic image of this particle starting at $R_1 = r_1 + nL_1$, where n is an integer number, arrives at $R_2 = r_2 + nL_2$. The difference of the naive displacements is $n\Delta L$, because Δr_f is the same for both images. Since n is arbitrary, this difference can be become arbitrarily large. In a periodic

TABLE 3: Thermodynamic Properties of the Mixtures

x (C_6 H_{10})	ρ_{sim} [kg/m^3]	ρ_{exp} [kg/m^3]	ΔH_{vap} [kJ/mol K]
0.000	767.7	772.1	32.94
0.023	768.7		32.93
0.250	777.4		32.87
0.500	783.1		32.58
0.750	793.4		32.51
0.977	800.6		32.31
1.000	802.7	805.0	32.38

[a] There is an uncertainty of 1 in the last digit.

system, properties must not depend on the choice of the periodic image, i.e., the origin of the coordinate system. Thus the effect of the rescaling step (the "scaling motion") must be eliminated.

There are several ways to do this or at least to limit its value to a well-defined border: Some authors fold the particle positions back into the central box, calculate the difference between the folded coordinates, and apply periodic boundary conditions on this difference to account for particles crossing the box boundary.[14] This method relies on the assumption that the particles do not move farther than half a box length between two saved configurations, which is easy to fulfill, and limits the "scaling motion" to a maximum of $\Delta L/2$.

We chose an alternative procedure: The displacement is calculated in *normalized* coordinates and then rescaled with the average of the two box sizes.

$$\Delta r = \bar{L}\left(\frac{r_2}{L_2} - \frac{r_1}{L_1}\right) \quad \text{with} \qquad \bar{L} = \frac{L_1 + L_2}{2} \tag{4}$$

This expression is translationally invariant, invariant under time reversal 1↔2, and it yields the correct result for constant L. It can easily be shown that the results for Δr obtained by the two methods differ by less than $\Delta L/2$ under the condition that

$$\left|\frac{r_2}{L_2} - \frac{r_1}{L_1} + \frac{|\Delta L|}{2\bar{L}}\right| < \frac{1}{2} \tag{5}$$

which is almost the same condition as the underlying assumption of the method described above.[14] We decided to use this method, because it is more plausible and needs less computational effort. In fact, the total displacement is equal to the displacement Δr_f rescaled with the average box size

$$\Delta r = \frac{\bar{L}}{L_1}\Delta r_f \tag{6}$$

This is sensible, because there is no a priori rule, in which order the two steps (propagation due to force and rescaling) have to be executed.

Results and Discussion

3.1. Thermodynamic Properties. The full configuration including positions and velocities of all atoms was saved every 1000th step (2 ps) during the simulation. This large interval guarantees that the values of the thermodynamic properties under examination are statistically independent, which was checked by inspecting their auto correlation functions. Those properties are the density ρ, which is calculated from the box size and the heat of vaporization $\Delta H_{vap} = -\langle E_{pot}^{inter}\rangle + RT$ from the intermolecular nonbonded energy. Table 3 shows these quantities for our mixtures. The density increases monotonically from 767.7 to 802.7 kg/m^3. The increase is almost linear, which is in agreement with experimental results (Figure 3). Note that the experiment was done at a lower temperature, thus there is an offset. ΔH_{vap} remains practically constant (no enthalpy of mixing). For the pure systems, the values match the experimental values, because the force field was optimized against them. The isothermal compressibility was calculated from volume fluctuations.[11] Its value is between 0.45 and 0.5 GPa^{-1}, which is far off the experimental values of 1.12 for cyclohexane[15] and 1.04 for cyclohexene.[16] We believe that this discrepancy may arise because the Berendsen manostat does not produce proper fluctuations, so that the fluctuation formula, which is valid for an *NpT* ensemble does not work correctly. To obtain reliable data, the compressibility must be calculated via finite differences between several pressures.[17] Since this is not the main subject of this study we refrained from further simulations.

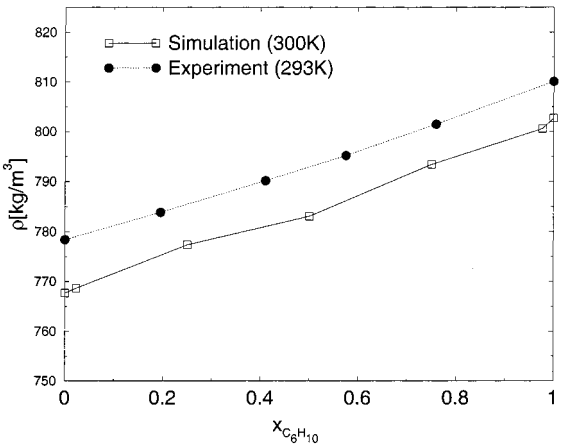

Figure 3. Density as a function of the molar fraction of cyclohexene in the simulation ($T = 300$ K) and experiment ($T = 293$ K).

3.2. Structure of the Mixture. The structure of a liquid mixture is not trivially deduced from the structures of its constituents. Therefore, radial distribution functions of the mixtures are investigated. Figure 4a shows radial distribution functions of the centers of mass of the molecules in the equimolar mixture.

One sees clearly that the system is fully mixed. The coordination of cyclohexene and cyclohexane is almost equal in the liquids. The cyclohexene molecules can approach more closely because they are smaller and additionally they are more anisotropic, so that there is a small probability to approach in a stacked conformation. Therefore, the peak for cyclohexene starts earlier. The structure is very similar to the one of pure liquids (Figure 4b). The coordination numbers, i.e., neighbors in the first shell, are shown in Table 4. At low cyclohexene concentration both components have slightly more cyclohexane neighbors than cyclohexene neighbors (if trivial effects of concentration are accounted for). At high cyclohexene concentrations both components have slightly more neighbors of the own type.

The radial distribution functions (RDF) of the carbon atoms in Figure 5 show the anisotropy and local structures of the molecules. The peaks of $g(r)$ of the molecules split up into several atomic peaks. The intramolecular part is neglected for clarity. There is a shoulder at smaller distances, so some carbons can approach each other more closely. The first molecular neighbor peak splits up into two, which resembles the atomistic structure. However, the second molecular neighbor peak can no longer be resolved into atomic peaks. The intermolecular radial distribution functions of the hydrogens (Figure 6) are indistinguishable between the pure liquids and the mixture if

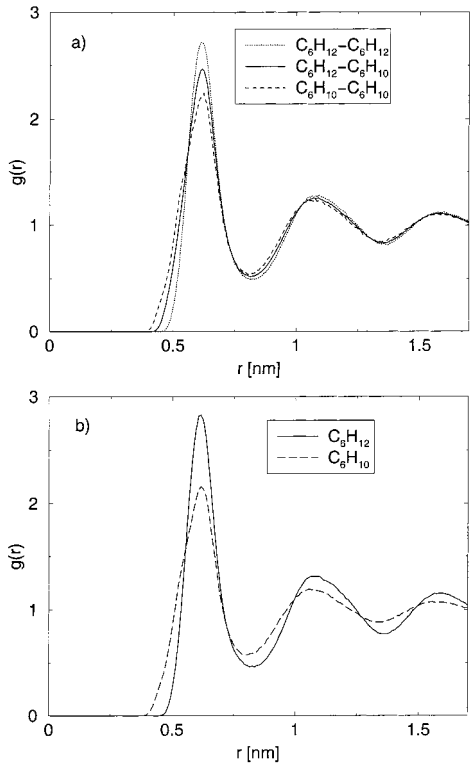

Figure 4. Radial distribution functions of the center of masses in (a) equimolar mixture and (b) pure liquids.

TABLE 4: Coordination Numbers in the First Neighbor Shell, Obtained by Integration of the Radial Distribution of the Centers of Mass Function to Its First Minimum[a]

$x(C_6H_{10})$	C_6H_{12}–C_6H_{12}	C_6H_{12}–C_6H_{10}	C_6H_{10}–C_6H_{12}	C_6H_{10}–C_6H_{10}
0.00	13.06			
0.25	9.86	3.23	9.70	3.16
0.50	6.34	6.32	6.32	6.18
0.75	3.37	9.49	3.16	9.52
1.00				12.69

[a] The table head means that the first component has *n* next neighbors of the second component, where *n* is denoted in the table.

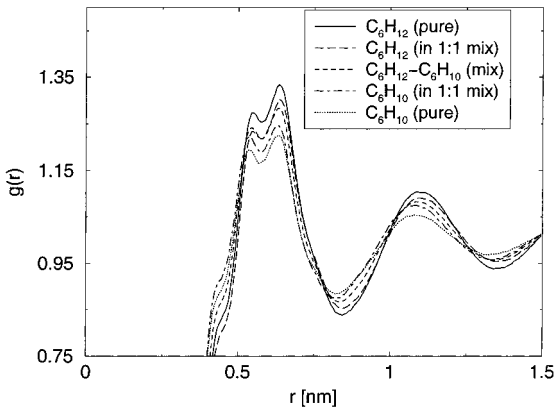

Figure 5. Intermolecular C−C radial distribution functions of pure liquids and 1:1 mixture. The plotted region is chosen to be able to show the differences of the curves.

one looks at cyclohexene or cyclohexane only. The interspecies RDF is easily explained by the average of the pure RDFs.

The structure of fully deuterated liquid cyclohexane was investigated experimentally by means of neutron diffraction by Farman et. al.[19] for different temperatures including our simulation temperature of 300 K. The difference between C_6H_{12} and C_6D_{12} is assumed to be negligible. To compare the results, we

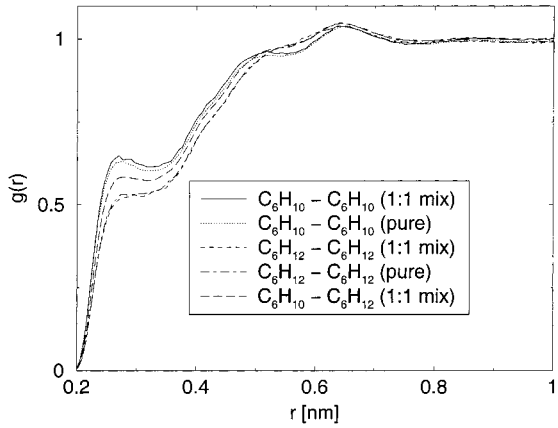

Figure 6. Intermolecular H−H radial distribution functions of pure liquids and 1:1 mixture.

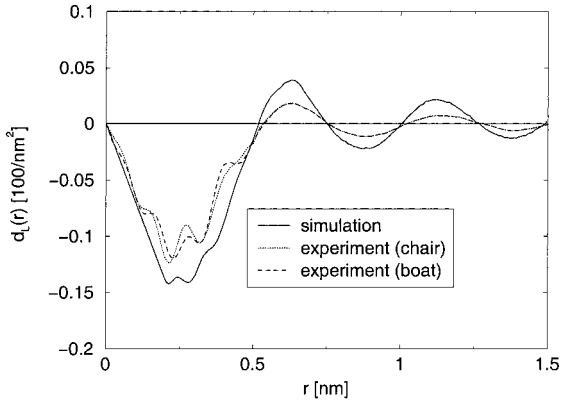

Figure 7. Comparison of the simulated cyclohexane structure to the experimental structure of deuterated cyclohexane gained by neutron diffraction[19] at 300 K.

show in Figure 7 the function

$$d_L(r) = 4\pi\frac{N}{V}[g(r) - 1] = 4\pi\frac{N}{V}[0.111g_{CC}(r) + 0.445g_{CH}(r) + 0.444g_{HH}(r) - 1] \quad (7)$$

after subtraction of the intramolecular parts together with the experimental data for 300K. The prefactors are due to the experimental scattering lengths of carbon and deuterium. The experiments are separately analyzed for the *boat* and the *chair* conformer.

The comparison shows satisfactory agreement. The main periods connected to the molecular size match very nicely. Also the fine structure of the first dip is reproduced. Therefore, our simulated liquid structure is quite realistic, although quantum effects have not been taken into account explicitly. However, since our force field has been developed for a particular state point, the potential may be regarded as an effective potential, which incorporates some quantum corrections implicitly.

3.3. Diffusion Coefficients. The diffusion coefficients in Table 5 and Figure 8 were calculated for all the mixtures as explained in section 2.3. For the *inter*diffusion coefficient the local exponent was allowed to be in the interval [0.8, 1.2], because the statistics is poor for the displacement of the center of mass. The inter diffusion coefficient can symmetrically be calculated from the center of mass motion of either species. Both values coincide within the given digits; this means that momentum is conserved quite accurately in the simulations. The errors given are the standard deviations of the "directional" diffusion coefficients D_x, D_y, and D_z. The experimental value

TABLE 5: Inter- and Intradiffusion Coefficients in 10^{-5} cm^2/s[a]

	D^{intra}		
$x(C_6H_{10})$	C_6H_{12}	C_6H_{10}	D^{inter}
0.000	0.89 ± 0.02		
0.023	0.84 ± 0.05	(0.95 ± 0.07)	0.73 ± 0.30
0.250	0.99 ± 0.03	1.15 ± 0.07	0.88 ± 0.06
0.500	1.09 ± 0.05	1.24 ± 0.16	1.26 ± 0.40
0.750	1.24 ± 0.11	1.34 ± 0.20	1.29 ± 0.30
0.977	1.43 ± 0.14	1.47 ± 0.07	1.46 ± 0.21
1.000		1.51 ± 0.09	

[a] Values in parantheses are unreliable because of poor statistics.

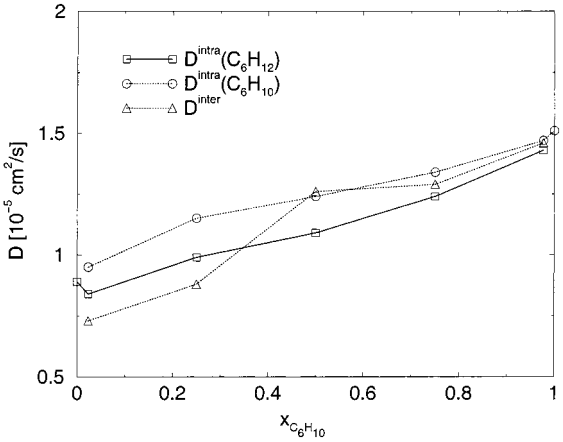

Figure 8. Diffusion coefficients, points are connected as a guide for the eye only.

for D^{intra} (C_6H_{12}) is 1.4×10^{-5} cm^2/s.[20] The intradiffusion coefficients of both components increase monotonically from pure cyclohexane to pure cyclohexene. This is probably due to the fact that cyclohexene is smaller than cyclohexane, which also leads to the difference in the viscosities[15] observed in experiments.

The calculated diffusion coefficients are noticeably smaller than the experimental diffusion coefficients for benzene−cyclohexane ($(1.8-2.1) \times 10^{-5}$ cm^2/s) and benzene−cyclohexene ($(2.1-2.4) \times 10^{-5}$ cm^2/s) mixtures.[21] Additionally, in the case of the mixture with benzene only an intermediate minimum is found and not the here observed multiple extrema with points of inflection in between.

However, mixtures of benzene with hexafluorobenzene show experimentally a similar characteristics of the diffusion coefficients including a point of inflection.[22] This behavior has been explained by a collective motion of molecules caused by association. Association is discussed in terms of velocity cross-correlation coefficients, which correlate motions of different molecules of one species or molecules of different species

$$f_{ij} = x_j \frac{N}{3} \int_0^\infty \mathrm{d}t \langle v_\alpha^i(0) v_\beta^j(t) \rangle, \quad \alpha \neq \beta \tag{8}$$

Here the average has to be taken over all different molecules α and β of species i and j, respectively. Note that f is an intensive quantity because the averaged correlation decays with $1/N$ for large N, since the number of uncorrelated velocities grows linearly.

These coefficients can alternatively be calculated from the diffusion coefficients.

$$f_{ij} = -\frac{x_j M_i M_j}{(x_i M_i + x_j M_j)^2} D^{inter}, \quad i \neq j \tag{9}$$

$$f_{ii} = \frac{x_j M_i^2}{(x_i M_i + x_j M_j)^2} D^{inter} - D_i^{intra} \tag{10}$$

For an ideal mixture (no preferred associations) with known diffusion coefficients the following cross-coefficients can be derived.[22,23]

$$f_{ij}^0 = -\frac{x_j M_i D_i^{intra}[1 + x_i \delta_{ij}]}{x_i M_i + x_j M_j} \tag{11}$$

$$f_{ii}^0 = -\frac{x_i M_i D_i^{intra}[1 - x_j \delta_{ij}]}{x_i M_i + x_j M_j} \tag{12}$$

with

$$\delta_{ij} = \frac{M_j D_j^{intra}}{M_i D_i^{intra}} - 1 \tag{13}$$

If we calculate the velocity cross-correlation coefficients according to eqs 9 and 10 and compare them to the corresponding values of the ideal mixture eqs 11 and 12, we find for low cyclohexene concentrations a strong discrepancy between the ideal and real behavior for the cyclohexene-cyclohexene interaction (Figure 9). This shows a stronger negative correlation than expected. The other functions are close to ideal. Thus, there is substantial deviation from ideality at low cyclohexene concentration, whereas in the high concentration regime there is no significance of nonideal behavior. This relates to the observation already mentioned that at low cyclohexene concentrations the cyclohexenes are in closer contact to cyclohexane molecules than to molecules of the same species.

3.4. Molecular Reorientation Dynamics. Molecular reorientation times can reveal aspects of local dynamic processes. They are defined via the decay of an orientation correlation function

$$A_n(t) = \langle P_n(\mathbf{u}(t)\mathbf{u}(0)) \rangle \tag{14}$$

where P_n is the nth order Legendre polynomial and $\boldsymbol{u}$ is a unit vector tied to the molecule. We considered the case $n = 1$ with $P_1 = \cos \alpha$. The decay times of the second and higher Legendre polynomials are shorter. In the Debye model of reorientation, $A(t)$ is expected to decay exponentially defining a decay time τ. The decay time of the second-order polynomial should be one-third of the one for the simple cosine. These assumptions are satisfied in our simulations if we focus on the C−C vectors (see Figure 10).

Both molecules are approximately oblate uniaxial ellipsoids, so that there are two natural choices of the unit vector: either a vector in the molecular plane or perpendicular to the plane. For reasons of simplicity and to compare our results with experiments, we investigated normalized distance vectors between suitably chosen atoms (Table 6), where possible. The reorientation of the axis itself ($\tau_\perp$) is investigated by a plane normal vector defined as follows. Atoms 1, 3, 5, and atoms 2, 4, 6 define planes with their respective normal unit vectors. The average of these unit vectors is taken as vector of the axis.

For cyclohexane, the parallel correlation time $\tau_{||}$ is measured for the C−C vectors across the ring (positions 1−4, 2−5, and 3−6). For cyclohexene, $\tau_{||}$ is measured from C_3 to C_6 which is across the ring just at the kink of the molecule. The *diagonal* reorientation time τ_d is measured across the ring from carbons at the double bond to the opposite side.

For both molecules, the reorientation times decrease with increasing cyclohexene concentration. The in-plane reorientation

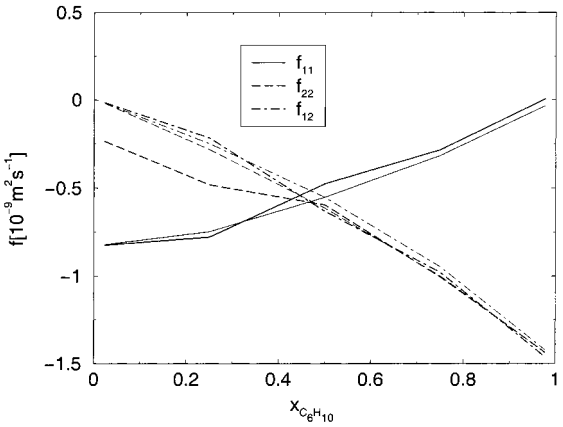

Figure 9. Comparison of velocity cross-correlation coefficients for the simulated system (thick lines) and a corresponding ideal system (thin lines). Index 1 indicates C_6H_{12}; 2 is C_6H_{12}.

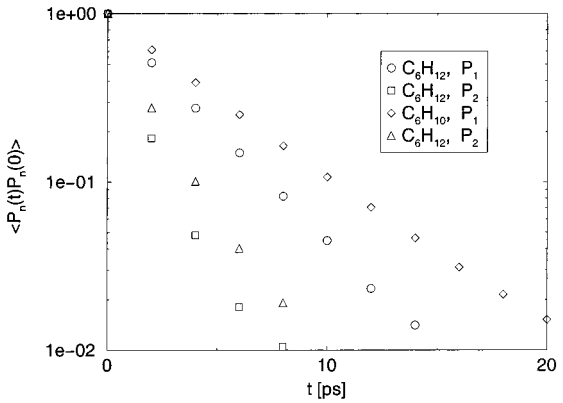

Figure 10. Decay of the autocorrelation function of Legendre polynomials of vectors across the ring (C_1-C_4) in the 1:1 mixture.

TABLE 6: Reorientation Times of Different Vectors in Picoseconds against the Mole Fraction of Cyclohexene

	cyclohexane			cyclohexene			
x (C_6H_{10})	$\tau_\parallel$	$\tau_\perp$	$\tau_\perp/\tau_\parallel$	$\tau_\parallel$	τ_d	$\tau_\perp$	$\tau_\perp/\tau_\parallel$
0.000	3.21	4.03	1.26				
0.023	3.20	4.08	1.28	4.31	4.60	5.50	1.28
0.250	3.18	3.89	1.22	4.49	4.74	5.53	1.23
0.500	3.12	3.64	1.17	4.16	4.54	5.25	1.26
0.750	2.94	3.60	1.22	4.17	4.47	5.11	1.20
0.997	2.98	3.26	1.09	4.08	4.39	5.00	1.23
1.000				4.13	4.43	4.97	1.20

[a] Additionally, the anisotropy between the slowest and fastest relaxation is shown.

is significantly faster than the reorientation of the plane. The reorientation times for cyclohexane are in satisfactory agreement with an NMR experiment using the spin−lattice relaxation time T_1 under the assumption of spherical reorientation.[24] There, the reorientation time of P_2 was found to be 1.27± 0.18ps. The average correlation time of P_2 in the simulation assumed Debye reorientation is 1.21ps.

Cyclohexene shows the same qualitative concentration dependence, but it is in general slower than cyclohexane. This agrees with the experimental finding that more anisotropic molecules reorient more slowly.[25]

There is a clear difference between in-plane rotation and the slower rotation of the molecular axis of cyclohexene. This result is in contradiction to another NMR experiment,[26] where a gaslike reorientation of cyclohexene was suggested. Their absolute values ($\tau_\parallel = 3.6$ ps and $\tau_\perp = 1.7$ ps) agree also only within the order of magnitude. However, our reorientation behavior seems to be more plausible in the liquid state. The simple argument that the reorientation times are determined only by the moment of inertia can only be applied to dilute, i.e., gas, phases. In a liquid phase, a reorientation of the molecular plane requires free volume, the surrounding molecules have to be displaced, while an in-plane rotation leaves the space occupied by the molecule almost unchanged. Thus an in-plane rotation meets less resistance by the liquid, so that it is faster than a rotation of the axis. This is supported by an NMR experiment on liquid cyclopentene.[25]

Additionally, the reorientation of the molecules becomes slightly more isotropic with increasing cyclohexene concentration. The anisotropic movement in the low concentration regime coincides with the more collective anti-correlated movement of the cyclohexene molecules we inferred from diffusion analysis. This supports that the mixture is closer to an ideal binary mixture with uncorrelated movement in the regime of higher cyclohexene concentration.

Concluding Remarks

Several mixtures of cyclohexane and cyclohexene were investigated in all-atom molecular dynamics simulations. The force field was constructed empirically from experimental thermodynamic data of the separate components. These force fields could reproduce additionally experimental data of structure and reorientation dynamics of the pure liquids.

The principal problem of calculation diffusion coefficients from *NpT* simulations was dealt with from a theoretical point of view. A plausible and simple expression for the calculation of the displacement from a trajectory was developed.

The *inter*- and *intra*diffusion coefficients were calculated. They show that the dynamics becomes faster with increasing cyclohexene concentration. This observation is in line with a decrease of the reorientation times of molecular vectors, which are in qualitative and partly in quantitative agreement with experiments. Moreover, molecular reorientation becomes more isotropic with increasing cyclohexene content. The reorientation and diffusion suggest a moderately collective motion of cyclohexene molecules at low cyclohexene concentration. The mixture comes closer to ideality in dynamical terms with increasing concentration of cyclohexene. The same trend is found in the local structure of the liquid.

Acknowledgment. We gratefully acknowledge stimulating discussions on the diffusion problem with Markus Deserno. We thank Andreas Dölle for sharing his experience in molecular reorientation.

References and Notes

(1) van Gunsteren, W. F.; Berendsen, H. J. C. *Angew. Chem., Int. Ed. Engl.* **1990**, *29*, 992−1023.

(2) Sun, H. *J. Phys. Chem. B* **1998**, *102*, 7338−7364.

(3) Mooney, D. A.; Müller-Plathe, F.; Kremer, K. *Chem. Phys. Lett.* **1998**, *294*, 135−142.

(4) McDonald, N. A.; Jorgensen, W. L. *J. Phys. Chem. B* **1998**, *102*, 8049−8059.

(5) Mittag, U.; Samios, J.; Dorfmüller, T. *Mol. Phys.* **1989**, *66*, 51−64.

(6) Kovacs, H.; Laaksonen, A. *J. Am. Chem. Soc.* **1991**, *113*, 5596−5605.

(7) Müller-Plathe, F. *Mol. Sim.* **1996**, *18*, 133−143.

(8) Woods, L. C. *Oxford Engineering Science;* Clarendon Press: Oxford, 1985; Vol. 2 (*The Thermodynamics of Fluid Systems*).

(9) Müller-Plathe, F. *Comput. Phys. Commun.* **1993**, *78*, 77−94.

(10) Berendsen, H. J. C.; Postma, J.; van Gunsteren, W.; DiNola, A.; Haak, J. *J. Chem. Phys.* **1984**, *81*, 3684−3690.

(11) Allen, M. P.; Tildesley, D. J. *Computer Simulation of Liquids;* Clarendon Press: Oxford, 1987.
(12) Faller, R.; Schmitz, H.; Biermann, O.; Müller-Plathe, F. *J. Comput. Chem.* **1999**, *20*, 1009−1017.
(13) Tyrrell, H. J. V.; Harris, K. R. *Diffusion in liquids: a Theoretical and Experimental Study;* Butterworth: London, 1984.
(14) Müller-Plathe, F. *Acta Polym.* **1994**, *45*, 259−293.
(15) Lide, D. R., Ed. *CRC Handbook of Chemistry and Physics*, 76th ed.; CRC Press: Boca Raton, 1995.
(16) Richard, A. J.; Flemming, P. B. *J. Chem. Thermodyn.* **1981**, *13*, 863−868.
(17) Paci, E.; Marchi, M. *J. Phys. Chem.* **1996**, *100*, 4314−4322.
(18) Landolt.; Börnstein. *Numerical Data and Functional Relationships in Science and Technology, New Series, Group IV*; Springer: Berlin, 1993; Vol. 1a.
(19) Farman, H.; Dore, J. C.; Bellisent-Funel, M.-C.; Montague, D. G. *Mol. Phys.* **1987**, *61*, 583−596.
(20) Landolt.; Börnstein. *Numerical Data and Functional Relationships in Science and Technology*, 6th ed., Springer: Berlin, 1983; Vol. 5a, Group II.
(21) Harris, K. R.; Dunlop, P. J. *Ber. Bunsen-Ges. Phys. Chem.* **1994**, *98*, 560−562.
(22) Weingärtner, H.; Braun, B. M. *Ber. Bunsen-Ges. Phys. Chem.* **1985**, *89*, 906−911.
(23) Mills, R.; Hertz, H. G. *J. Phys. Chem.* **1980**, *84*, 220−224.
(24) O'Reilly, D. E.; Peterson, E. M.; Hogenboom, D. L. *J. Chem. Phys.* **1972**, *57*, 3969−3976.
(25) Grant, D. M.; Pugmire, R. J.; Black, E. P.; Christensen, K. A. *J. Am. Chem. Soc.* **1973**, *95*, 8465−8466.
(26) Pajak, Z.; Latanowicz, L.; Jurga, K. *Ber. Bunsen-Ges. Phys. Chem.* **1980**, *84*, 769−775.